

Current status of oxide clusterfullerenes[‡]

Laura Abella^a, Yaofeng Wang^b, Antonio Rodríguez-Forte^{a,*}, Ning Chen^{b,*}, Josep M. Poblet^{a,*}

^aDepartament de Química Física i Inorgànica, Universitat Rovira i Virgili, c/Marcel·lí Domingo 1, 43007 Tarragona, Spain.

^bLaboratory of Advanced Optoelectronic Materials, College of Chemistry, Chemical Engineering and Materials Science, Soochow University, Suzhou, Jiangsu, 215123, China.

[‡]Dedicated to Prof. L. Echegoyen on occasion of his 65th anniversary.

KEYWORDS: Fullerene, Endohedral, Oxide cluster, Scandium, DFT

ABSTRACT: The field of endohedral metallofullerenes has developed extraordinarily since the synthesis and characterization of $\text{Sc}_3\text{N}@I_h\text{-C}_{80}$ in 1999, the third most abundant fullerene after C_{60} and C_{70} . During these almost two decades other clusterfullerenes have been trapped inside different IPR and non-IPR fullerenes. Sc_2O has demonstrated to be a good template for middle size fullerenes, between C_{70} and C_{82} , permitting to characterize many structures and determining different physical properties. This mini-review will allow the reader to gain insight into the field of endohedral metallofullerenes and in particular into the richness of the fullerenes containing scandium oxide clusters as well as into experimental and theoretical techniques used to characterize them.

Contents

1. Introduction
2. Sc_2O , a promiscuous cluster for fullerenes
 - 2.1 Structural characteristics
 - 2.2 Motion of the Sc_2O cluster inside the fullerenes
 - 2.3 Cage connectivity for $\text{Sc}_2\text{O}@C_{2n}$ family ($2n=70$ to 82)
 - 2.4 Comparison $\text{Sc}_2\text{O}@C_{2n}$ vs $\text{Sc}_2\text{S}@C_{2n}$
3. $\text{Sc}_4\text{O}_3@C_{80}$, the clusterfullerene containing the largest number of atoms, and other $I_h\text{-C}_{80}$ OCFs
4. Redox properties of scandium oxide clusterfullerenes
 - 4.1 Electrochemical Studies
 - 4.2 Prediction of the redox potentials and correlation with the electronic structure
5. ⁴⁵Sc NMR studies of scandium oxide clusterfullerenes
6. Conclusions

1. Introduction

Endohedral fullerenes have attracted much attention due to its unique capacity of encapsulating different species inside the hollow fullerene cage.[1, 2] These fullerenes are of special interests because of their endohedral chemistry and applications in the field of molecular electronic devices,[3, 4] organic solar cells[5-9] and biomedicine.[10, 11] To date, various species, including atoms,[12-16] metal ions,[17, 18] clusters[19-24] and small molecules,[25] have been successfully encapsulated into fullerene cages by different synthetic methods. Among them, clusterfullerenes (CFs) have become the focus of the recent studies, due to their tunable encapsulated structures, high stabilities and relatively high yields. Until now, most of lanthanide metals have been entrapped into the fullerene cages in form of variable clusters. Very recently, Ti and V based CFs were also reported.[26-28] Various families of clusterfullerenes have been synthesized and characterized, such as nitride,[19, 27, 29-33] carbide,[23, 24, 34-39] hydrocarbide,[40] carbon nitride,[41] sulfide,[26, 42-44] and oxide[20-22, 45-47] families. Interestingly, the molecular structures of most of these CFs intend to follow a somewhat fixed template. For example, nitride clusterfullerenes (NCFs) family is one of the largest families of CFs. However, all the NCFs reported to date followed a trimetallic nitride template, which was first found and proposed by Dorn et al.[48] Sulfide clusterfullerenes (SCFs), on the other hand, follows a dimetallic sulfide template, in which two metal and one sulfur atom form the encapsulated cluster.[42] Oxide clusterfullerenes (OCFs), however, present versatile encapsulated structures that broke the template rule. The first reported OCF is $\text{Sc}_4\text{O}_2@I_h\text{-C}_{80}$ (31924), followed by the discovery of $\text{Sc}_4\text{O}_3@I_h\text{-C}_{80}$ (31924), which still remains the record as CF with the largest cluster ever entrapped inside fullerenes.[47, 49] These two OCFs shared the same $I_h\text{-C}_{80}$ cage with a six-electron metal-to-cage charge transfer, similar to those found for NCFs. Interestingly, in 2010, Stevenson et al. reported a dimetallic OCF, $\text{Sc}_2\text{O}@C_s\text{-C}_{82}$ (39715).[47] This OCF demonstrated similar structure and physicochemical properties as SCF $\text{Sc}_2\text{S}@C_s\text{-C}_{82}$ (39715).[50] The above three structures reported by Stevenson et al. show that OCFs could be versatile both in the encapsulated clusters and the fullerene cages. However, the extensive family members of OCFs were yet to be explored. Recently, we reported a novel synthetic method for the preparation of an extensive family of OCFs. With the introduction of CO_2 as oxygen source, a modified arc-discharging method was used and a large family of $\text{Sc}_2\text{O}@C_{2n}$ ($n=35\text{-}45$) were produced and detected by mass spectrum (MS).[45] Followed by the successful synthesis, we were able to isolate $\text{Sc}_2\text{O}@C_{2\text{-}C_{70}}$ (7892),[45] $\text{Sc}_2\text{O}@T_d\text{-C}_{76}$ (19151),[46] $\text{Sc}_2\text{O}@D_{3h}\text{-C}_{78}$ (24109), $\text{Sc}_2\text{O}@C_{2v}\text{-C}_{78}$ (24107),[22] $\text{Sc}_2\text{O}@C_{2v}\text{-C}_{80}$ (31922),[21] and $\text{Sc}_2\text{O}@C_{3v}\text{-C}_{82}$ (39717),[20] the single crystal structures of all these OCFs were characterized for the first time and their physicochemical properties have been fully investigated. In addition, a unique paramagnetic OCF, $\text{Sc}_3\text{O}@C_{80}$ was isolated and studied by DFT calculations.[51] This is the very first time that a large family of CFs with extensive cage structures has been fully characterized. The combined theoretical and experimental studies of these structures show that the cages of these OCFs are correlated with each other. The shapes of the encapsulated dimetallic oxide clusters were also found to be affected by the cage structures. Furthermore, the influence of both cages and clusters on the electrochemical properties of these fullerenes were revealed. Thus, to better understand the correlation between molecular structures and physicochemical properties of the OCFs, in this work, we provided a detailed and comprehensive overview of the current studies of OCFs for the first time. The molecular structures and cluster dynamics of these OCFs were discussed extensively including the structures of some missing OCFs, such as $\text{Sc}_2\text{O}@C_{74}$ and $\text{Sc}_4\text{O}_4@C_{80}$, which were proposed and studied by DFT calculations. Based on these results, the structural connectivities between fullerene cages of $\text{Sc}_2\text{O}@C_{2n}$ ($2n=70$ to 82) were revealed. In addition, the electrochemical properties and the ^{45}Sc NMR studies of these OCFs were summarized to understand the impact of the fullerene cages on their physicochemical properties.

2. Sc₂O, a promiscuous cluster for fullerenes

2.1. Structural characteristics

Several fullerenes containing a metal oxide cluster such as Sc₂O, Sc₄O₂, Sc₄O₃ have been synthesized and characterized by single-crystal X-ray crystallography.[20-22, 46, 47] The Sc₂O unit, which is the smallest endohedral cluster found inside fullerenes, along with M₂S and MCN clusters, and larger than endohedral monometal or dimetal units, has been found in a large number of carbon cages. Most of the cages in the range of 70-84 carbon atoms have been characterized by X-ray crystallography: Sc₂O@C₂-C₇₀(7892), Sc₂O@T_d-C₇₆(19151), Sc₂O@C_{2v}-C₇₈(24107), Sc₂O@D_{3h}-C₇₈(24109), Sc₂O@C_{2v}-C₈₀(31922), Sc₂O@C_s-C₈₂(39715) and Sc₂O@C_{3v}-C₈₂(39718). Their optimized structures are shown in Figure 1. The predicted cages for those Sc₂O@C_{2n} that have not been isolated yet, Sc₂O@C_s-C₇₂(10528), Sc₂O@D_{3h}-C₇₄(14246), Sc₂O@C₂-C₇₄(13333), Sc₂O@C_{2v}-C₈₄(51575) and Sc₂O@C₁-C₈₄(51580) are also represented in Figure 1.

The Sc₂O cluster always transfers four electrons to the fullerene cages. This kind of oxide cluster generally adopts a bent structure when it is encapsulated inside a fullerene. All Sc₂O@C_{2n} isomers fulfill the isolated pentagon rule with the only exception of three of them, whose structures show the pentalene motifs highlighted in orange in Figure 1. These three non-IPR isomers have two adjacent pentagon pairs (APP) with the Sc atoms of the cluster pointing to them. For those IPR cages, different orientations of the Sc₂O unit can be found. The lowest energy orientation of the cluster for each isomer is shown in Figure 1.

Table 1 shows the most characteristic (computed and experimental) structural parameters for the Sc₂O@C_{2n} family, such as distances and angles within the Sc₂O cluster. Although not always the two Sc-O bond lengths in the Sc₂O unit have the same value, the averages of both Sc-O distances in each Sc₂O@C_{2n} cage are comparable among them, having a range of 1.880-1.927 Å. Computed values, albeit somewhat smaller, are in good agreement with the experimental ones. The Sc-O bond length is rather constant regardless of the cage size. The Sc₂O@C_{3v}-C₈₂(39717) and Sc₂O@C_{2v}-C₈₀(31922) isomers have the shortest and largest Sc-O distances, respectively (1.875 and 1.933 Å). The largest computed Sc-O-Sc angle is found in the hypothetical Sc₂O@C_s-C₇₂(10528) cage (167.0°). This largest Sc-O-Sc angle is consequence of the peculiar structure this non-IPR cage. Both scandium atoms are pointing to the two pentalene motifs, thus the angle is less compressed than in other cages. Something similar happens to Sc₂O@C₂-C₇₀(7892), where the Sc-O-Sc angle (139.6 comp. and 131.2 degrees exp.) is mainly dictated by the position of the two pentalene motifs in the cage. The computed Sc-C distances are also rather constant regardless of the size of the cage, meaning that this cluster fits well inside cages in the range of C₇₀ to C₈₄. As Table 1 shows, the largest Sc-O-Sc angles are found for larger cages, although still nonlinear geometries are commonly observed. The variations of the Sc-O-Sc angle within the cluster among the Sc₂O@C_{2n} family indicate that there is some kind of influence of the cage structure on the endohedral cluster shape. The dimetallic oxide cluster, Sc₂O, inside the carbon cages is extremely flexible, i.e., it can rotate freely inside the cage and the angular shape is very flexible (*vide infra*). Thus, the shape and the size of the cages play a role in the Sc-O-Sc angle that the cluster adopts.

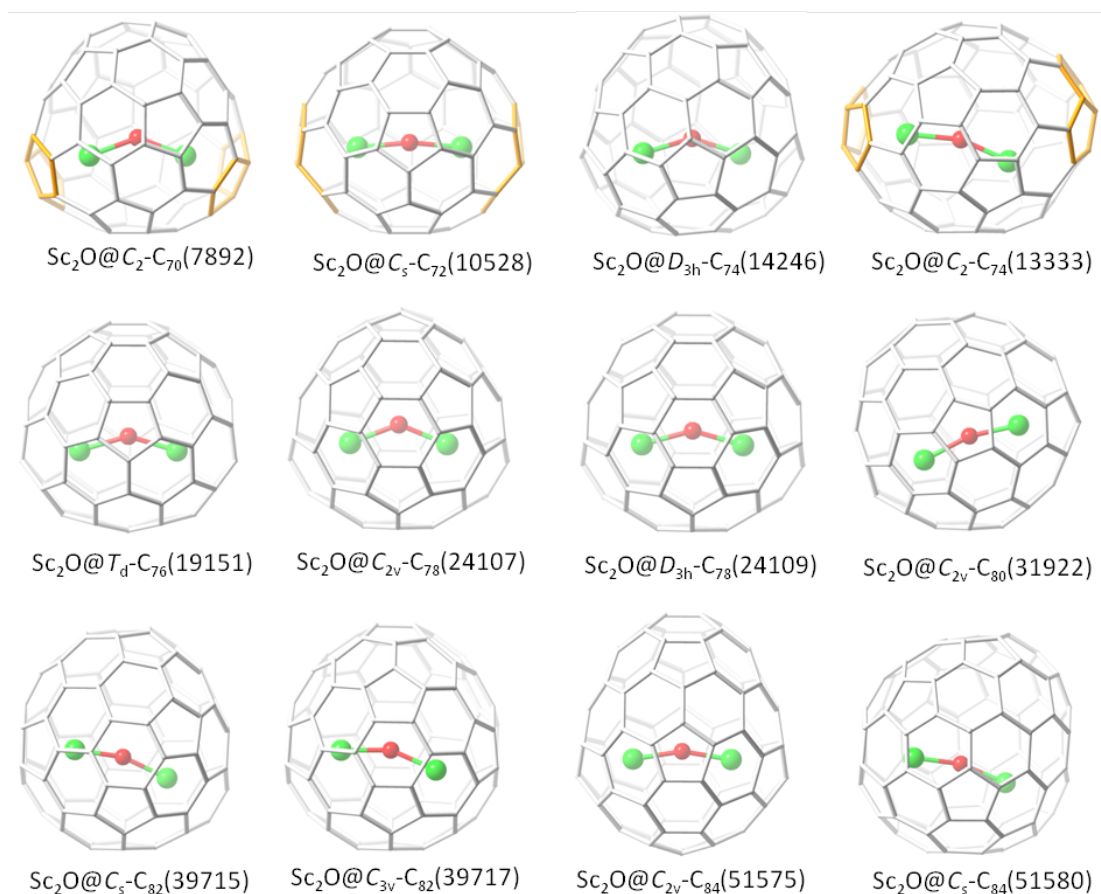


Figure 1. DFT-optimized structures of X-ray characterized and predicted most abundant isomers for each $\text{Sc}_2\text{O}@C_{2n}$ with n from 35 to 42.

Table 1. Computed and experimental X-ray values for Sc-O distances (in Å) and Sc-O-Sc angles (in degrees), the average of Sc-cage (Sc-C) distances (in Å) and the Sc-Sc distances (in Å) for the $\text{Sc}_2\text{O}@C_{2n}$ family.

Isomer	Sc1-O comp	Sc1-O exp	Sc2-O comp	Sc2-O exp	Sc-Sc comp	Sc-C comp	Sc-O-Sc comp	Sc-O-Sc exp
C_2-C_{70} (7892)	1.881	1.909	1.881	1.931	3.531	2.374	139.6	131.2
C_5-C_{72} (10528)	1.928	-	1.926	-	3.830	2.452	167.0	-
C_2-C_{74} (14246)	1.888	-	1.892	-	3.614	2.397	146.0	-
$D_{3h}-C_{74}$ (13333)	1.923	-	1.876	-	3.747	2.402	161.0	-
T_d-C_{76} (19151)	1.883	1.972	1.884	1.825	3.611	2.421	146.9	133.9
$C_{2v}-C_{78}$ (24107)	1.879	1.905	1.880	1.868	3.501	2.308	137.2	134.4
$D_{3h}-C_{78}$ (24109)	1.887	1.903	1.887	1.979	3.633	2.320	148.7	135.2
$C_{2v}-C_{80}$ (31922)	1.896	1.861	1.933	2.017	3.792	2.414	164.2	160.8
C_5-C_{82} (39715)	1.881	1.867	1.911	1.943	3.747	2.379	162.2	156.6
$C_{3v}-C_{82}$ (39717)	1.888	1.937	1.875	1.888	3.673	2.371	154.8	131.0-148.9
$C_{2v}-C_{84}$ (51575)	1.883	-	1.881	-	3.714	2.400	161.3	-
C_1-C_{84} (51580)	1.905	-	1.873	-	3.746	2.385	165.0	-

2.2. Motion of the Sc₂O cluster inside the fullerenes

Car-Parrinello molecular dynamics simulations at room temperature and 2000 K, a temperature near to the one reached in fullerene formation, have been performed to gain more insight about the motion of the Sc₂O cluster inside the Sc₂O@C_{2n} fullerenes. The motion of the cluster depends importantly on the simulation temperature (see Figure 2). Significant variations of (i) Sc1-O-Sc2 angles and (ii) relative orientations of the cluster at room temperature are observed, thus free rotation of the Sc₂O cluster is operative on the NMR time scale. In all the systems analyzed, the major motion of the Sc₂O cluster is observed in C_{3v}-C₈₂(39717) cage, which shows that the cluster can rotate and change the Sc1-O-Sc2 angle easily at rather low temperature. At 2000 K, the oscillations of the angle and distances are much more important, which confirms the high flexibility of the Sc₂O unit inside the corresponding cages. The averages and standard deviations for the Sc1-O-Sc2 angles and Sc-O distances at the two simulated temperatures, 298 and 2000 K, are represented in Table 2. There is almost no difference between the average Sc1-O distance and average Sc2-O distance for all the OCFs analyzed. These results also corroborate the high flexibility of the cluster inside the D_{3h}-C₇₄(14246), T_d-C₇₆(19151), C_{2v}-C₈₀(31922) and C_{3v}-C₈₂(39717) cages. Although the Sc₂O unit is very flexible and freely moving inside the fullerene cage, its angular shape is kept around the average angle, i.e. no linear arrangement of the cluster is observed.

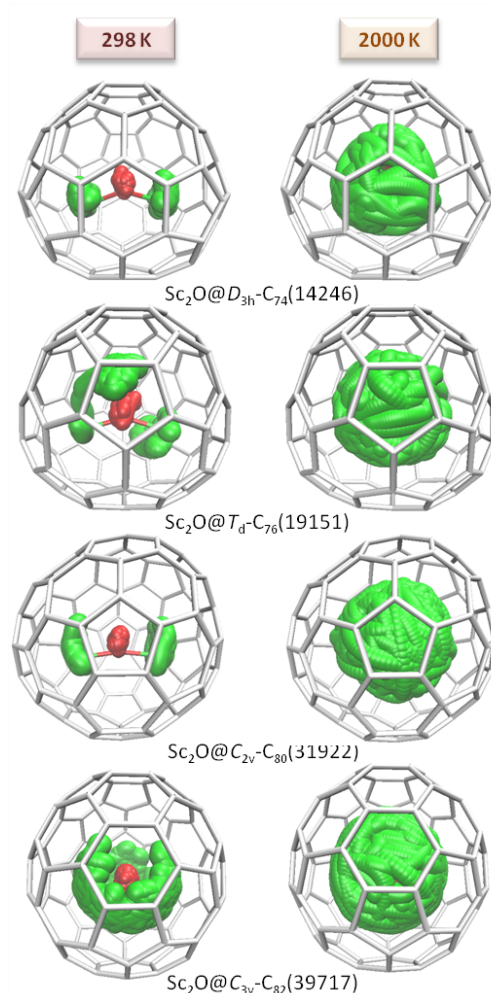


Figure 2. Representation of the motion of the Sc₂O cluster inside the D_{3h}-C₇₄(14246), T_d-C₇₆(19151), C_{2v}-C₈₀(31922) and C_{3v}-C₈₂(39717) cages during the Car-Parrinello molecular dynamics trajectories at room temperature and 2000 K.

Table 2. The average of the Sc1-O-Sc2 angles (degrees) and Sc-O distances (in Å) for the Sc₂O@C_{2n} cages along their Car-Parrinello trajectories at 298 and 2000 K. Standard deviations are shown in parenthesis.

Isomer	Sc1-O-Sc2	Sc-O
298 K		
<i>D</i> _{3h} -C ₇₄ (14246)	135 (7)	1.99 (0.03)
<i>T</i> _d -C ₇₆ (19151)	131 (7)	2.04 (0.04)
<i>C</i> _{2v} -C ₈₀ (31922)	155 (10)	2.01 (0.03)
<i>C</i> _{3v} -C ₈₂ (39717)	147 (8)	1.99 (0.03)
2000 K		
<i>D</i> _{3h} -C ₇₄ (14246)	139 (14)	2.00 (0.05)
<i>T</i> _d -C ₇₆ (19151)	134 (17)	2.05 (0.07)
<i>C</i> _{2v} -C ₈₀ (31922)	146 (17)	2.01 (0.06)
<i>C</i> _{3v} -C ₈₂ (39717)	147 (18)	2.02 (0.06)

2.3. Cage connectivity for Sc₂O@C_{2n} family (2n=70 to 82)

Although many efforts have been devoted to understand fullerene formation, the mechanism is still unclear and under debate.[52-56] Many theoretical studies have suggested that the formation of fullerenes could follow a “top-down” mechanism.[57-60] In this sense, Dorn and coworkers have shown that graphene sheets can roll and warp to form fullerenes under electron beam irradiation following a “top-down” mechanism.[61] On the other hand, studies on the more classical “bottom-up” mechanism have been reported providing many insights into fullerene formation. Nowadays, it is assumed that in presence of a rich carbon atmosphere a closed fullerene can grow likely following a relatively simple mechanism.[57, 58] At low carbon concentrations, it is likely that Stone-Wales (SW) (or similar) rearrangements are dominant and the less stable structures are transformed to give the thermodynamic product in most cases.

Figure 3 shows a growth scheme for the Sc₂O@C_{2n} family through C₂ additions and SW transformations assuming the mechanism proposed by Endo and Kroto in the early nineties and denominated later as Closed Network Growth (CNG) mechanism.[62-64] The critical point of this mechanism is that the fullerenes formed after a C₂ addition does not obey the isolated pentagon rule due to the formation of two fused pentagonal rings. In particular, here we show that Sc₂O@C₂-C₇₀(7892) and Sc₂O@C_{3v}-C₈₂(39717) are linked by six C₂ insertions plus a few number of SW transformations for some of the isomers. The initial two cages C₂-C₇₀(7892) and C₅-C₇₂(10528) do not satisfy the IPR, but after the second insertion the most favorable isomers for each cage are of the IPR type and therefore it is needed at least one SW rearrangement to transform the non-IPR isomer into an IPR.

As mentioned, the first step relates cages C₂-C₇₀(7892) and C₅-C₇₂(10528) through a simple C₂ insertion (see Figure 3). Once the C₂ unit is inserted into the selected hexagon of Sc₂O@C₂-C₇₀(7892), Sc₂O@C₅-C₇₂(10528) is formed. Although the C₅-C₇₂(10528) cage has been detected encapsulating Sc₂S, it has not been still found encapsulating a scandium oxide. However, it would also be the optimal isomer to capture Sc₂O. The next step is the formation of Sc₂O@*D*_{3h}-C₇₄(14246) from Sc₂O@C₅-C₇₂(10528) through the C₂ insertion and two SW transformations. *D*_{3h}-C₇₄(14246) has been observed encapsulating Sc₂O neither, but it has been detected hosting a Sc₂C₂ cluster.[23] A detailed structural path from C₂-C₇₀(7892) to *D*_{3h}-C₇₄(14246) has been reported for Sc₂S@C_{2n} by Fowler and co-workers.[65] Next step corresponds to the formation of Sc₂O@*T*_d-C₇₆(19151) from C₂ insertion into Sc₂O@*D*_{3h}-C₇₄(14246) followed by a SW transformation. Then, the two observed cages with 78 carbon atoms containing a Sc₂O cluster can be connected with Sc₂O@*T*_d-C₇₆(19151) by C₂ insertion plus one or two SW transformations. Indeed, these two cages, C₇₈(24109) and C₇₈(24107), are related by a single SW rearrangement.[22] The following step relates isomer Sc₂O@C_{2v}-C₈₀(31922) with Sc₂O@C_{2v}-C₇₈(24107) and Sc₂O@*D*_{3h}-C₇₈(24109) through a C₂ insertion and one or two SW transformations. Finally, the largest observed C₈₂ cages, C₅-C₈₂(39715) and C_{3v}-C₈₂(39717) can be formally derived

from $\text{Sc}_2\text{O}@C_{2v}\text{-C}_{80}(31922)$, even though the cage with symmetry C_{3v} would require 4 SW transformations. Likely, $\text{Sc}_2\text{O}@C_{2v}\text{-C}_{80}(31922) \rightarrow \text{Sc}_2\text{O}@C_{2v}\text{-C}_{82}(39717)$ occurs via non-classical intermediates containing a heptagonal ring.[24, 66]

To summarize, the observed cages for OCFs are linked via C_2 insertions and few SW rearrangements. This is not specific for these OCFs since other clusterfullerenes containing tetravalent units, Sc_2S^{4+} or $\text{Sc}_2\text{C}_2^{4+}$, display rather similar connections. The greatest advantage of the $\text{Sc}_2\text{O}@C_{2n}$ family with respect to other families is the number of observed species that allow a more detailed analysis of the real links between the different species.

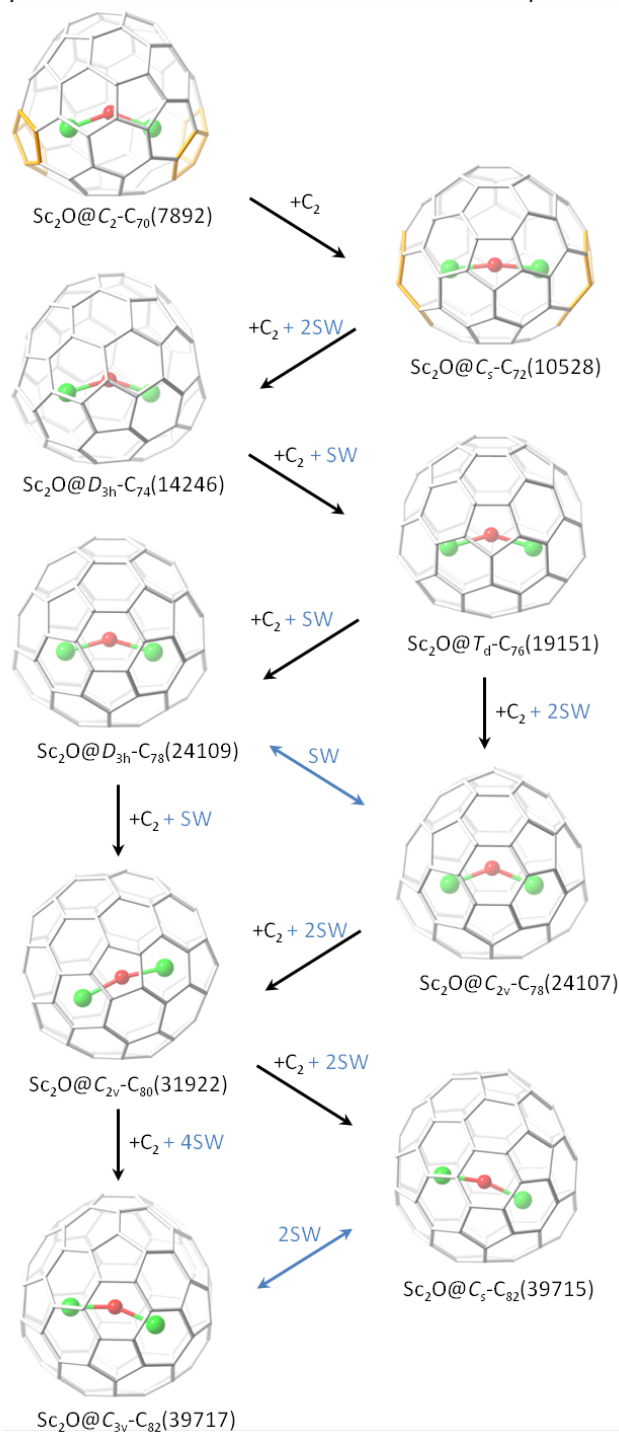


Figure 3. Structural connections among the $\text{Sc}_2\text{O}@C_{2n}$ family. Arrows in black indicate a simple C_2 insertion and blue represent a Stone-Wales (SW) transformation (see Figure S1 for a detailed description of each step).

2.4. Comparison $\text{Sc}_2\text{O}@C_{2n}$ vs $\text{Sc}_2\text{S}@C_{2n}$

Sulfur and oxygen belong to the same group of the periodic table (chalcogens) and, consequently, they have the same number of valence electrons. Therefore, the clusters that they can form by combination with metals can be very similar. Indeed, just before Stevenson, Poblet and Balch characterized the structure of the first Sc_2O -based OCF, $\text{Sc}_2\text{O}@C_5\text{-C}_{82}$ (39715),[67] in 2010 Yang, Popov and Dunsch had isolated and characterized the family of sulfide clusterfullerenes (SCFs) $\text{M}_2\text{S}@C_{3v}\text{-C}_{82}$ (39717) with $\text{M} = \text{Sc}, \text{Y}, \text{Dy}$ and Lu by using solid guanidinium thiocyanate as sulfur source.[68] In 2011, a collaboration between the groups of Stevenson, Echegoyen, Poblet and Balch resulted in the synthesis (SO_2 as sulfur source) and characterization of the electrochemical properties and the structures of $\text{Sc}_2\text{S}@C_5(6)\text{-C}_{82}$ and its isomer $\text{Sc}_2\text{S}@C_{3v}(8)\text{-C}_{82}$. [50] Later in 2012, Balch, Poblet and Echegoyen isolated and characterized $\text{Sc}_2\text{S}@C_5\text{-C}_{72}$ (10528), which was the first dimetallic sulfide clusterfullerene with a non-IPR cage, as shown by X-ray crystallography.[43] Finally, in 2013, Poblet and Echegoyen found that the Sc_2S cluster could also be encapsulated in another small and non-IPR C_{70} cage, $\text{Sc}_2\text{S}@C_2\text{-C}_{70}$ (7892).[44] Even though the structure was not determined by X-ray crystallography, electrochemical and spectroscopic characterization, as well as complementary DFT calculations doubtlessly pointed to $C_2\text{-C}_{70}$ (7892) to be the cage present in this SCFs. Besides these isolated SCFs, the mass spectra showed peaks for a large number of members within the $\text{Sc}_2\text{S}@C_{2n}$ family, ranging from $2n = 68$ to 100.[42] Structures for some of these peaks have been proposed from computations.[69, 70]

Sulfide and oxide clusterfullerenes of the type $\text{Sc}_2\text{X}@C_{2n}$ ($\text{X} = \text{O}, \text{S}$) share identical electronic structures with formal electron transfers of four electrons from the cluster to the cage.[71, 72] Therefore, the most favored fullerene cages that are predicted to encapsulate Sc_2O and Sc_2S are, according to the ionic model, the same. In fact, most of the cages that have been observed to contain Sc_2S they have been also found for Sc_2O . Since the sulfide anion is larger than the oxide anion, the Sc-S distances within the cluster are larger than the corresponding Sc-O distances (see Tables 3 and 1). Therefore, the larger Sc_2S cluster has to bend more the Sc-S-Sc angle to fit well inside the same cages that encapsulate the smaller Sc_2O cluster. Hence, Sc-S-Sc angles in SCFs are significantly smaller than Sc-O-Sc angles in OCFs (see Tables 3 and 1). Finally, the predicted very similar electronic structure for $\text{Sc}_2\text{S}@C_{2n}$ and $\text{Sc}_2\text{O}@C_{2n}$ was confirmed by computations of the frontier molecular orbital energies. The HOMO energies of SCFs and OCFs, as well as their LUMO energies, are quite similar with differences smaller than 40 mV that are consequence of the different nature of the cluster and interaction with the C_{2n} cage. Besides, the shapes of these frontier molecular orbitals are essentially the same for sulfides and oxides (see Figure 4). The calculated oxidation and reduction potentials are able to reproduce the small changes observed in the cyclic voltammetry experiments, i.e. it is somewhat easier to oxidize and reduce the oxide than the sulfide for $C_2\text{-C}_{70}$ (7892) and $C_5\text{-C}_{82}$ (39715), while it is slightly easier to oxidize and reduce the sulfide for $C_{3v}\text{-C}_{82}$ (39717). Even though the electrochemical (EC) gaps are computed with a given error, which can be up to 230 mV for the $\text{Sc}_2\text{X}@C_2\text{-C}_{70}$ (7892) systems, the differences between the EC gaps between the sulfide and the oxide CFs are very well reproduced in all the cases: +140 (calc) vs +120 mV (exp) for $C_2\text{-C}_{70}$ (7892), +60 (calc) vs +60 mV (exp) for $C_5\text{-C}_{82}$ (39715) and -150 (calc) vs -150 mV (exp) for $C_{3v}\text{-C}_{82}$ (39717).

Table 3. Computed and experimental values for Sc-S distances (in Å) and Sc-S-Sc angles (in degrees) for the $\text{Sc}_2\text{S}@C_{2n}$ family.

Isomer	Sc1-S comp	Sc1-S exp	Sc2-S comp	Sc2-S exp	Sc-S-Sc comp	Sc-S-Sc exp
$C_2\text{-C}_{70}$ (7892)	2.352	-	2.352	-	97.8	-
$C_5\text{-C}_{72}$ (10528)	2.345	2.325	2.345	2.347	124.4	125.4
$C_5\text{-C}_{82}$ (39715)	2.350	2.353	2.370	2.390	113.6	113.8
$C_{3v}\text{-C}_{82}$ (39717)	2.360	2.335	2.360	2.416	105.3	97.3

Table 4. Electronic structure parameters computed at BP86/TZP level along with experimental and computed oxidation and reduction potentials for several $\text{Sc}_2\text{S}@C_{2n}$ and $\text{Sc}_2\text{O}@C_{2n}$ systems.

	$C_2-C_{70}(7892)$		$C_5-C_{82}(39715)$		$C_{3v}-C_{82}(39717)$	
	Sc_2S	Sc_2O	Sc_2S	Sc_2O	Sc_2S	Sc_2O
HOMO	-4.79	-4.75	-5.01	-4.98	-5.17	-5.19
LUMO	-3.84	-3.88	-4.17	-4.16	-3.98	-3.96
H-L gap	0.95	0.87	0.84	0.82	1.19	1.23
$E_{\text{ox,calc}}$	0.04	-0.02	0.24	0.19	0.42	0.45
$E_{\text{red,calc}}$	-1.33	-1.25	-0.99	-0.98	-1.07	-1.19
EC_{calc}	1.37	1.23	1.23	1.17	1.49	1.64
$E_{\text{ox,exp}}$	0.14	0.10	0.39	0.35	0.52	0.54
$E_{\text{red,exp}}$	-1.44	-1.36	-0.98	-0.96	-1.04	-1.17
EC_{exp}	1.58	1.46	1.37	1.31	1.56	1.71

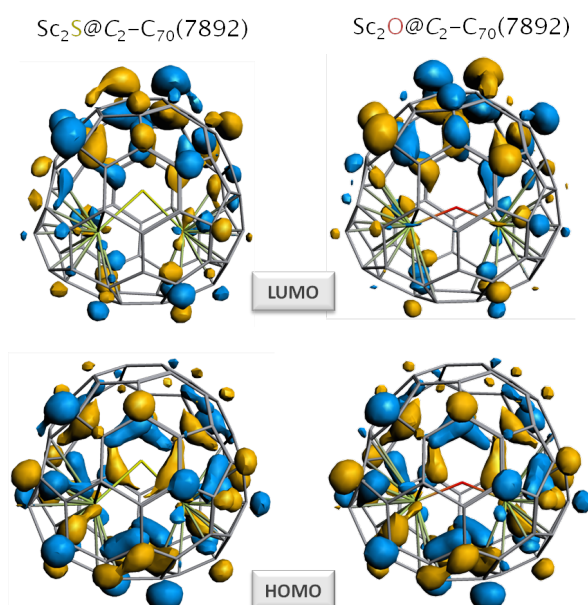


Figure 4. Representation of the HOMO and LUMO for $\text{Sc}_2\text{S}@C_2-C_{70}(7892)$ and $\text{Sc}_2\text{O}@C_2-C_{70}(7892)$, which are very similar in the two systems.

3. $\text{Sc}_4\text{O}_3@C_{80}$, the clusterfullerene containing the largest number of atoms, and other I_h-C_{80} OCFs

Besides Sc_2O , which can be encapsulated in many different carbon cages, other scandium oxide clusters with larger number of metals, such as Sc_4O_2 , Sc_4O_3 , and recently Sc_3O , have been also found, all of them inside the prototypical I_h-C_{80} cage. $\text{Sc}_4\text{O}_2@I_h-C_{80}$ was the first OCF isolated and characterized.[47] $\text{Sc}_4\text{O}_3@I_h-C_{80}$ is, along with $\text{Sc}_3\text{C}_2\text{CN}@I_h-C_{80}$, the clusterfullerene that encapsulates the largest number of atoms.[73, 74] The trimetallic oxide $\text{Sc}_3\text{O}@I_h-C_{80}$ is a quite special clusterfullerene that was obtained in rather high quantity in the raw soot, but most of it remained nonextracted in the soot so that only a small amount of it was isolated and purified.[51] According to the ionic model,[71, 72] all these OCFs can be regarded as $(\text{OC})^{6+}@I_h-C_{80}^{6-}$, where OC stands for oxide cluster, in contrast to the formal four electron transfer in $(\text{Sc}_2\text{O})^{4+}@C_{2n}^{4-}$. The clusters $\text{Sc}_4(\mu_3\text{-O})_2$ and $\text{Sc}_4(\mu_3\text{-O})_3$, with tri-coordinated oxide anions, share the same type of cubane-like structure where the four Sc ions are placed in the vertexes of a

distorted tetrahedron and the two, or three, oxide anions above the centre of two, or three, faces, i.e. in the remaining vertexes of the cube (see Figure 5). Interestingly, Sc...Sc distances within Sc_4O_2 cluster show larger variability than those within Sc_4O_3 , a fact that is intimately related to the different electronic structures of these two clusterfullerenes (see Table 5 and *vide infra*). Sc_3O is, however, a planar equilateral triangular cluster with the oxide anion in the middle of the triangle, isostructural to Sc_3N . Computational studies have shown that these clusters, which are rather compact even though they contain up to six or seven atoms, can rotate quite freely inside the spherical $I_h\text{-C}_{80}$ cage.[75]

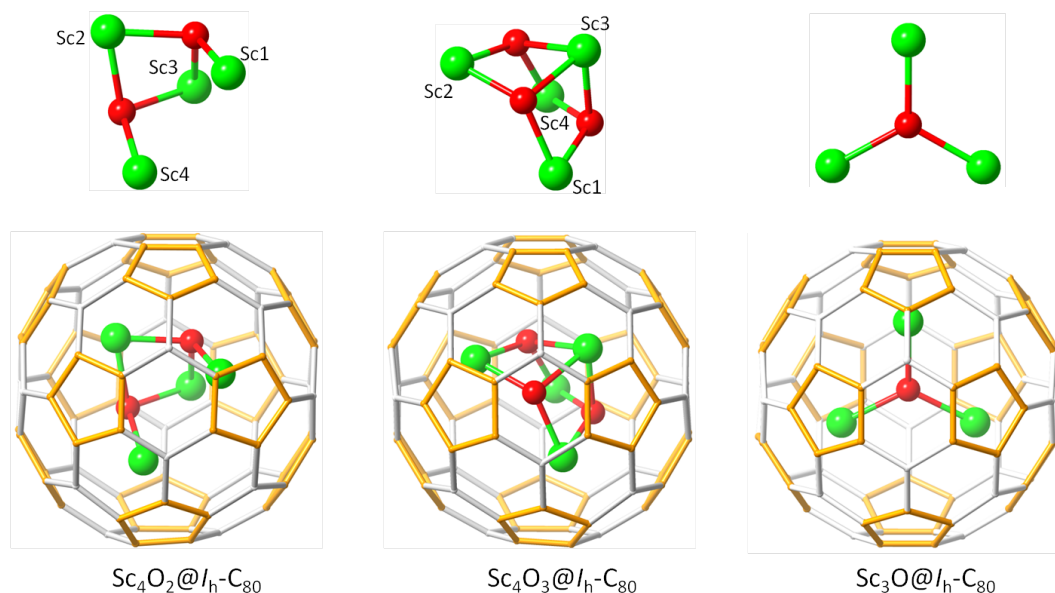


Figure 5. Optimized structures of $\text{Sc}_4\text{O}_2@I_h\text{-C}_{80}$, $\text{Sc}_4\text{O}_3@I_h\text{-C}_{80}$ and $\text{Sc}_3\text{O}@I_h\text{-C}_{80}$. The geometries of the cluster, with the Sc atom properly numbered, are shown in the upper part of the figure.

Table 5. Computed and experimental Sc-Sc and Sc-O distances for $\text{Sc}_4\text{O}_x@I_h\text{-C}_{80}$ ($x=2$ and 3).^a

	$\text{Sc}_4\text{O}_2@I_h\text{-C}_{80}$			$\text{Sc}_4\text{O}_3@I_h\text{-C}_{80}$	
	Calc	Exp		Calc	Exp
Sc2-Sc3	2.96	2.95	Sc2-Sc ^c	2.98	3.01
Sc1-Sc4	3.21	3.12	Sc-Sc ^d	3.45	3.43
Sc-Sc ^b	3.29	3.30			
Sc-O	2.01	2.05	Sc-O	1.99	1.99

^a Distances in Å; ^b Average of the Sc1-Sc2, Sc1-Sc3, Sc2-Sc4 and Sc3-Sc4 distances in Sc_4O_2 ; ^c Average of the three short Sc2-Sc distances in Sc_4O_3 : Sc2-Sc3, Sc2-Sc1 and Sc2-Sc4; ^d Average of the three long Sc-Sc distances in Sc_4O_3 : Sc1-Sc3, Sc1-Sc4 and Sc3-Sc4.

The electronic distributions for these OCFs are somewhat different for each of them. The simplest one corresponds to $(\text{Sc}^{3+})_4(\text{O}^{2-})_3@I_h\text{-C}_{80}^{6-}$, with four Sc^{3+} ions. However, the situation is different in $(\text{Sc}^{3+})_2(\text{Sc}^{2+})_2(\text{O}^{2-})_2@I_h\text{-C}_{80}^{6-}$, with two Sc^{3+} and two Sc^{2+} ions. In the latter, the HOMO is largely confined to the $\text{Sc}_4(\mu_3\text{-O})_2$ unit, while in $\text{Sc}_4(\mu_3\text{-O})_3@I_h\text{-C}_{80}$ the HOMO is largely delocalized over the fullerene carbon atoms, as in $\text{Sc}_3\text{N}@I_h\text{-C}_{80}$. [76] Representations of the HOMOs for these two OCFs are given in Figure 6. Looking closer at the HOMO of $\text{Sc}_4(\mu_3\text{-O})_2@I_h\text{-C}_{80}$, one can realize that it is mainly located between two Sc ions (Sc1 and Sc4 in the original X-ray structure), bearing each of them one electron and thus becoming formally Sc^{2+} ions. This idea, first proposed by Rodriguez-Forte and Poblet [76] and later confirmed by Popov and Dunsch by means of analysis of the topology of the electronic density based on the quantum theory of atoms in molecules (QTAIM), [77] was in striking contrast with the original proposal by Stevenson et al. who suggested that the short distance between Sc3 and Sc4 in the experimental structure was an indication of bonding between these two Sc atoms. The LUMOs for these two

OCFs are mainly located in the oxide cluster and show quite similar energies (Figure 6). The relative high energy of the HOMO in $\text{Sc}_4(\mu_3\text{-O})_2@I_h\text{-C}_{80}$ located in the cluster, leads to a HOMO-LUMO (HL) gap of only 0.60 eV, a value that is rather small compared to the one in $\text{Sc}_4(\mu_3\text{-O})_3@I_h\text{-C}_{80}$, 1.48 eV (Figure 6). Besides, the oxidation potential for $\text{Sc}_4(\mu_3\text{-O})_2@I_h\text{-C}_{80}$ is predicted to be very low, -0.09 V, in good agreement with experiment (0.00 V).[49] The first oxidation potential for $\text{Sc}_4(\mu_3\text{-O})_3@I_h\text{-C}_{80}$ is, however, predicted to be at a much more positive value, 0.58 V. The EC gap, directly related to the HL gap, for $\text{Sc}_4(\mu_3\text{-O})_2@I_h\text{-C}_{80}$ is computed to be very small, 0.88 V, in good agreement with experiment, 1.10 V. In contrast, the EC gap for $\text{Sc}_4(\mu_3\text{-O})_3@I_h\text{-C}_{80}$ is predicted to be significantly larger, 1.68 V, in accordance with its larger HL gap.[76]

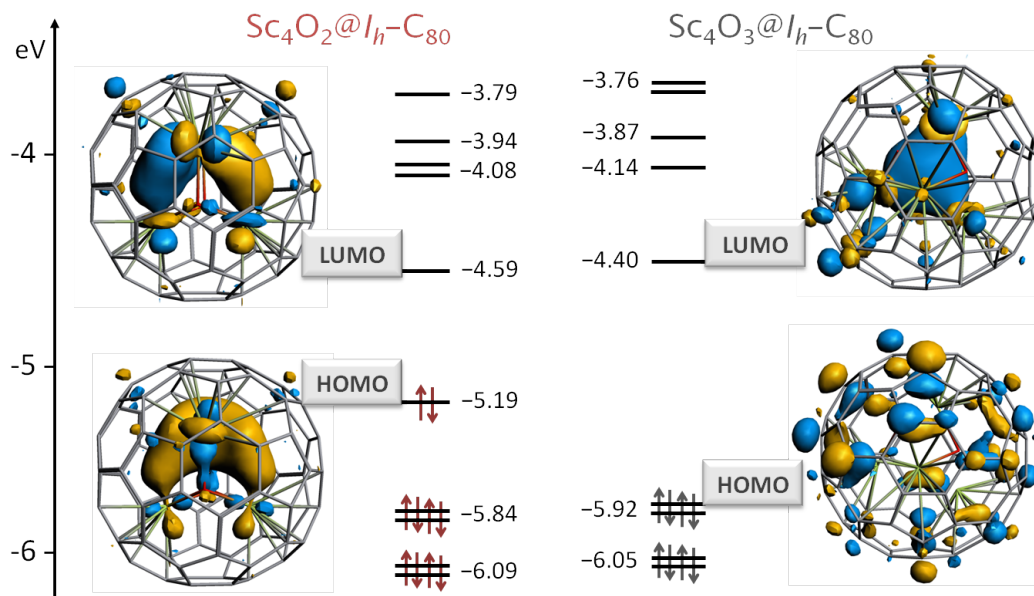


Figure 6. Molecular orbital diagrams and representations of the HOMO and LUMO for $\text{Sc}_4(\mu_3\text{-O})_2@I_h\text{-C}_{80}$ and $\text{Sc}_4(\mu_3\text{-O})_3@I_h\text{-C}_{80}$.

The special characteristics of the frontier molecular orbitals of $\text{Sc}_4(\mu_3\text{-O})_3@I_h\text{-C}_{80}$ (LUMO) and $\text{Sc}_4(\mu_3\text{-O})_2@I_h\text{-C}_{80}$ (HOMO and LUMO), which are localized on the oxide cluster, make them clusterfullerenes with endohedral electrochemical activity, i.e. with redox processes *in cavea*. [78] For $\text{Sc}_4(\mu_3\text{-O})_3@I_h\text{-C}_{80}$, even though it has been isolated and crystallized, no electrochemical characterization has been done so far. The endohedral electrochemical activity was demonstrated, however, for $\text{Sc}_4(\mu_3\text{-O})_2@I_h\text{-C}_{80}$ by Popov, Dunsch and Echegoyen by means of an in situ electron spin resonance (ESR) spectroelectrochemical study of the spin density distribution in the electrochemically generated cation and anion radicals.[49] The Sc-based hyperfine structure with large hyperfine coupling constants that they found showed that both oxidation and reduction on this OCF take place *in cavea*. Spin densities on the cation and anion radicals of $\text{Sc}_4(\mu_3\text{-O})_2@I_h\text{-C}_{80}$, localized on the oxide cluster, had already been predicted by Rodriguez-Forteza and Poblet (see Figure 7).[76]

The electronic distribution of the recently characterized $\text{Sc}_3\text{O}@I_h\text{-C}_{80}$ is also different as those in the cubane-like $\text{Sc}_4\text{O}_x@I_h\text{-C}_{80}$ ($x=2, 3$) clusterfullerenes.[51] The system presents an odd number of electrons, i.e. it is a radical. The unpaired electron is distributed equivalently among the three Sc ions leading, within the ionic model, to $(\text{Sc}_3)^{3+}\text{O}^{2-}@I_h\text{-C}_{80}^{6-}$, with three formally $\text{Sc}^{2.67+}$ ions. $\text{Sc}_3\text{O}@I_h\text{-C}_{80}$ is isoelectronic with the anion $\text{Sc}_3\text{N}@C_{80}^-$, as well as the characteristic mixed-metal nitride $\text{TiSc}_2\text{N}@C_{80}$. Both the LUMO and the SOMO (singly occupied molecular orbital), which is the highest occupied molecular orbital in systems with unpaired electrons, as well as the spin density, are localized in the Sc_3O cluster (see Figure 7). Therefore, both electrochemical oxidation and reduction are expected to take place in the endohedral oxide as for $\text{Sc}_4(\mu_3\text{-O})_2@I_h\text{-C}_{80}$.

C_{80} . The first oxidation potential for $Sc_3O@I_h-C_{80}$ is predicted to be at -0.42 V, a very low value compared to other OCFs (see Table 7). The lowest anodic potential for an OCF measured so far is 0.00 V for $Sc_4(\mu_3-O)_2@I_h-C_{80}$ (computed value of -0.09 V, vide supra). On the other side, the predicted reduction potential, -1.16 V, is comparable to those for $Sc_2O@C_{3v}-C_{82}$ (39717) (-1.19 V) and somewhat more cathodically shifted than for other OCFs (Table 7). Consequently, the predicted EC gap for $Sc_3O@I_h-C_{80}$, 0.74 V, which is significantly small, is the lowest gap among all the OCFs known so far. Unfortunately, the tiny quantity of pure product acquired made not possible the electrochemical characterization. A plausible explanation for this tiny quantity of purified product compared to the rather high abundance of this OCF in the raw soot has been proposed. It is known that some pristine fullerene cages that are free radicals or have small H-L gaps, i.e., with kinetic instability, are prone to polymerize forming insoluble products that are difficult to extract from raw soot using organic solvents. Computed reaction energies for the formation of different $[Sc_3O@I_h-C_{80}]_2$ dimers show that dimerization is a favourable process for this radical OCF.

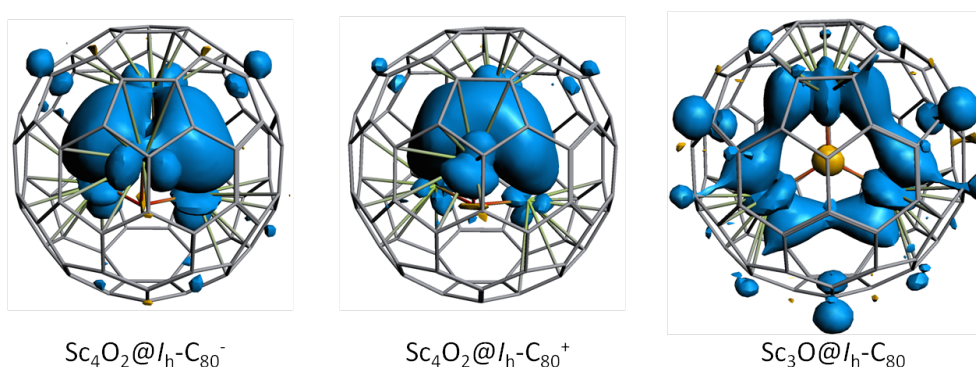


Figure 7. Spin-density distributions for the anion and cation radicals of $Sc_4O_2@I_h-C_{80}$ and neutral $Sc_3O@I_h-C_{80}$.

To conclude this section, we would like to comment on the hypothetical cubane oxide clusterfullerenes, $Sc_4O_4@C_{2n}$, recently proposed by Rodriguez-Forteza and Poblet as candidates to be detected in near future experiments.[75] Even though this kind of OCFs would contain as much as eight atoms inside the fullerene cage, the cubane cluster is rather compact, even more compact than distorted cubes in $Sc_4O_x@I_h-C_{80}$ ($x = 2$ and 3). According to the ionic model, we can see the cubane oxide clusterfullerenes as $(Sc_4^{3+})(O_4^{2-})@(C_{2n})^{4-}$, with a formal transfer of four electrons from the cluster to the cage. Therefore, this hypothetical family of OCFs would share structure with distorted cubanes $Sc_4O_x@I_h-C_{80}$ ($x = 2$ and 3) and electronic structure with $Sc_2O@C_{2n}$ systems (see Figure 8). $C_{3v}-C_{82}$ (39717), which is the prototypical cage to encapsulate clusters with charge transfers of four electrons, as well as $C_{2v}-C_{82}$ (39718) are predicted to encapsulate Sc_4O_4 . The Sc–O and Sc···Sc distances within the cubane in isomers $C_{3v}-C_{82}$ (39717) and $C_{2v}-C_{82}$ (39718) are essentially the same as for the characterized $Sc_4O_3@I_h-C_{80}$, indicating that the 8-atom cubane fits well inside these two C_{82} cages with no compression in the intracluster distances compared to the 7-atom oxide. In addition, the Sc···C shortest contacts in the hypothetical $Sc_4O_4@C_{82}$ fullerenes are significantly longer (average distances of 2.44 and 2.42 Å for isomers $C_{3v}-C_{82}$ (39717) and $C_{2v}-C_{82}$ (39718), respectively) than for $Sc_4O_3@I_h-C_{80}$ (2.28 Å), corroborating that the cubane 8-atom oxide fits well inside C_{82} . Both HOMO and LUMO are localized on the cage for the two $Sc_4O_4@C_{3v}-C_{82}$ (39717) and $Sc_4O_4@C_{2v}-C_{82}$ (39718) systems, in contrast to $Sc_4O_3@I_h-C_{80}$ (see Figure 8). Therefore, it is not expected the electrochemistry to take place in cavea. The H-L gap for $Sc_4O_4@C_{3v}-C_{82}$ (39717) (1.04 eV) is much larger than for $Sc_4O_4@C_{2v}-C_{82}$ (39718) (0.44 eV), so the former would be kinetically more stable.

Encapsulation of the cubane oxide is also predicted inside T_d-C_{76} (19151), even though the cage is six C atoms smaller than C_{82} . The compactness of the cubic Sc_4O_4 cluster allows it to fit well

inside the tetrahedral T_d - C_{76} (19151) cage. The HOMO and the LUMO are mainly localized on the cage, as for $Sc_4O_4@C_{82}$ systems, and the H-L gap (0.94 eV) is as large as that found for $Sc_4O_4@C_{3v}$ - C_{82} (39717) (1.04 eV), confirming that the electronic structure of the T_d - C_{76} (19151) cage is suitable to accept four electrons (vide infra).

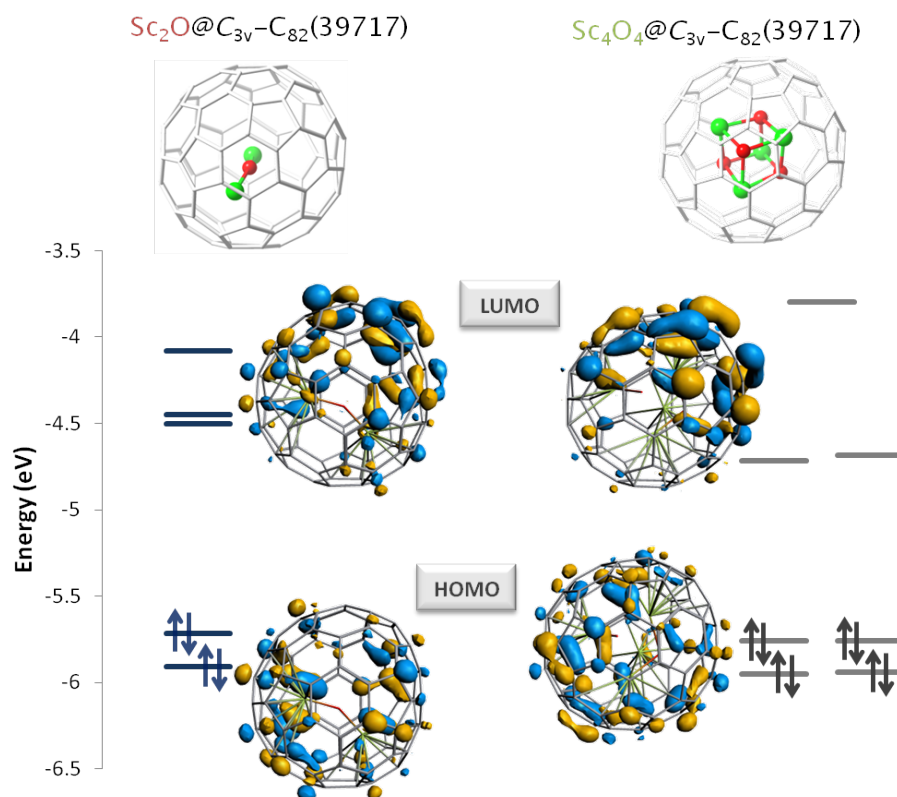


Figure 8. Optimized structures, orbital diagrams and representations of HOMO and LUMO for $Sc_2O@C_{3v}$ - C_{82} (39717) and $Sc_4O_4@C_{3v}$ - C_{82} (39717).

4. Redox properties of scandium oxide clusterfullerenes

4.1. Electrochemical Studies

The electrochemical behavior of scandium-based metallic OCFs, $Sc_4O_2@I_h$ - C_{80} and $Sc_2O@C_{2n}$ ($n=35,38,79,40,41$), have been studied extensively, which provides a unique opportunity to evaluate the impact of cage size and symmetry on the electrochemical properties of a clusterfullerene family.

$Sc_2O@C_2$ - C_{70} (7892) was identified as the smallest and the only non-IPR OCF reported so far.[45] On one hand, $Sc_2O@C_2$ - C_{70} (7892) has an exceptionally lower first oxidation potential (0.10 V) compared to those of the other dimetallic OCFs, which suggests it has the best electron-donating ability among the reported dimetallic OCFs. On the other hand, this OCF demonstrates far more negative first reduction potential (-1.36 V) than other members of OCFs family, indicating its poor electron-accepting ability.

The first oxidation process and first reduction process of $Sc_2O@T_d$ - C_{76} (19151)_[46] are reversible. Similar electrochemical behavior and redox potentials were also observed for $Sc_2O@C_s$ - C_{82} (39715)_[79]. In addition, the overall redox processes of these two dimetallic OCFs resemble each other very much. Though computational studies suggested that the redox processes of both $Sc_2O@T_d$ (19151)- C_{76} and $Sc_2O@C_s$ (39715)- C_{82} are cage-based, the similar electrochemical

behaviors of these two OCFs suggest that the different cage structures did not bring a major change to their redox processes.

Interestingly, the electrochemical behavior of $\text{Sc}_2\text{O}@D_{3h}\text{-C}_{78}$ (24109) did not show much resemblance to that of its isomeric counterpart, $\text{Sc}_2\text{O}@C_{2v}\text{-C}_{78}$ (24107), even though their cage structures are closely related by a SW transformation.[22] The $\text{Sc}_2\text{O}@D_{3h}\text{-C}_{78}$ (24109) shows fully reversible reduction waves, whereas the reduction process of $\text{Sc}_2\text{O}@C_{2v}\text{-C}_{78}$ is completely irreversible. But in the anodic region, the first oxidation process of $\text{Sc}_2\text{O}@D_{3h}\text{-C}_{78}$ (24109) and $\text{Sc}_2\text{O}@C_{2v}\text{-C}_{78}$ (24107) are reversible and have almost identical value. These results correlate with the DFT results that show that $\text{Sc}_2\text{O}@D_{3h}\text{-C}_{78}$ (24109) and $\text{Sc}_2\text{O}@C_{2v}\text{-C}_{78}$ (24107) have rather similar HOMOs but some difference exist between their LUMOs. Moreover, the electrochemical gap of $\text{Sc}_2\text{O}@D_{3h}\text{-C}_{78}$ (24109) is 0.85 V, which is the smallest gap among the OCFs discovered so far.

The redox behaviors of another two isomeric structures, $\text{Sc}_2\text{O}@C_s\text{-C}_{82}$ (39715) and $\text{Sc}_2\text{O}@C_{3v}\text{-C}_{82}$ (39717) again, show major differences.[20, 79] The first oxidation and the first reduction processes of $\text{Sc}_2\text{O}@C_s\text{-C}_{82}$ (39715) are reversible, while the first reduction process of $\text{Sc}_2\text{O}@C_{3v}\text{-C}_{82}$ (39717) is irreversible. Similar difference was observed between $\text{Sc}_2\text{O}@D_{3h}\text{-C}_{78}$ (24109) and $\text{Sc}_2\text{O}@C_{2v}\text{-C}_{78}$ (24107). These results indicated that the difference of cage symmetry of the isomers has a strong influence on their electronic structure. On the other hand, the first oxidation potential and the first reduction peak potentials of $\text{Sc}_2\text{O}@C_{3v}\text{-C}_{82}$ (39717) are 0.54 V and -1.17 V respectively, which result in an electrochemical gap of 1.71 eV, the largest among the OCFs.

A trend could be observed for $\text{Sc}_2\text{O}@C_{2n}$, except for $\text{Sc}_2\text{O}@T_d\text{-C}_{76}$ (19151), that the first oxidation potential of the OCFs shift cathodically with the increase of their cage size. The reduction potentials are more complicated as there is no obvious trend that could be concluded, which is in line with their dramatically different LUMO energy levels. Furthermore, the electrochemical studies of OCFs also shows that that the symmetry of carbon cage have a significant impact on the electrochemical properties, as the two isomers of $\text{Sc}_2\text{O}@C_{82}$ and $\text{Sc}_2\text{O}@C_{78}$ show dramatically different redox behavior respectively.

The CV of $\text{Sc}_4\text{O}_2@I_h\text{-C}_{80}$ is reversible in both reductive and oxidative processes, which is remarkable considering the irreversible reductive behaviors for most of CFs. The redox potential of this OCF is also rather special as the first oxidation step appears at 0.00 V. Further detailed computational analysis showed the first oxidation happened as one electron was removed from the Sc-Sc bonding HOMO, which is different from the fact that most of the HOMOs of dimetallic OCFs are essentially cage based.

Table 6. Redox potentials (V vs Fc^+/Fc) for scandium-based oxide endohedral cluster fullerenes obtained in $(n\text{-Bu}_4\text{N})(\text{PF}_6)/o\text{-dcb}$ with ferrocene as the internal standard.

OCF	$E^{2+/+}$	$E^{+/0}$	$E^{0/-}$	$E^{-1/2}$	$E^{-2/3}$	$E^{-3/4}$	$E^{-4/5}$	EC	ref
$\text{Sc}_2\text{O}@C_2\text{-C}_{70}$ (7892)	0.55 ^a	0.10 ^a	-1.36 ^b	-1.80 ^b				1.46	[45]
$\text{Sc}_2\text{O}@T_d\text{-C}_{76}$ (19151)		0.32 ^a	-0.91 ^a	-1.40 ^b	-1.65 ^b	-1.93 ^a	-2.30 ^b	1.23	[46]
$\text{Sc}_2\text{O}@C_{2v}\text{-C}_{78}$ (24107)	0.64 ^a	0.16 ^a	-1.17 ^b	-1.66 ^b	-1.93 ^b			1.33	[22]
$\text{Sc}_2\text{O}@D_{3h}\text{-C}_{78}$ (24109)	0.62 ^c	0.18 ^a	-0.67 ^a	-0.86 ^a				0.85	[22]
$\text{Sc}_2\text{O}@C_{2v}\text{-C}_{80}$ (31922)	0.56 ^a	0.24 ^a	-0.89 ^b	-1.48 ^b	-1.75 ^b	-1.96 ^b	-2.13 ^b	1.13	[21]
$\text{Sc}_2\text{O}@C_s\text{-C}_{82}$ (39715)	0.72 ^a	0.35 ^a	-0.96 ^a	-1.28 ^a	-1.74 ^a			1.31	[79]
$\text{Sc}_2\text{O}@C_{3v}\text{-C}_{82}$ (39717)	1.09 ^b	0.54 ^a	-1.17 ^b	-1.44 ^b	-1.55 ^b	-1.78 ^b		1.71	[20]
$\text{Sc}_4\text{O}_2@I_h\text{-C}_{80}$ (31924)	0.79 ^{a,d}	0.00 ^{a,d}	-1.10 ^{a,d}	-1.73 ^{a,d}	-2.35 ^{b,d}			1.10	[80]

^aHalf-wave potential in volts (reversible redox process). ^bPeak potential in volts (irreversible redox process). ^cCyclic Voltammogram (DPV) potentials. ^dOsteryoung Square Wave Voltammetry (OSWV)

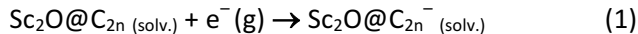
4.2. Prediction of the redox potentials and correlation with the electronic structure

Table 7. Computed and experimental (V vs Fc⁺/Fc) first oxidation and reduction potentials, electrochemical (EC) gaps, HOMO and LUMO energies and HOMO-LUMO (H-L) gaps for some Sc₂O@C_{2n} OCFs.^{a)}

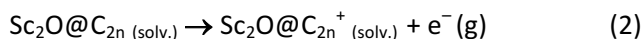
OCF	E _{ox,calc}	E _{red,calc}	EC _{calc}	E _{ox,exp}	E _{red,exp}	EC _{exp}	HOMO	LUMO	H-L gap
C ₂ -C ₇₀ (7892)	-0.02	-1.25	1.23	0.10	-1.36	1.46	-4.75	-3.88	0.86
C ₅ -C ₇₂ (10528)	0.15	-1.19	1.34	-	-	-	-4.90	-3.96	0.95
C ₂ -C ₇₄ (14246)	-0.08	-0.89	0.81	-	-	-	-4.67	-4.27	0.40
T _d -C ₇₆ (19151)	0.15	-1.00	1.15	0.32	-0.91	1.23	-4.93	-4.15	0.78
C _{2v} -C ₇₈ (24107)	0.02	-1.13	1.15	0.16	-1.17	1.33	-4.77	-4.01	0.76
D _{3h} -C ₇₈ (24109)	0.02	-0.70	0.72	0.18	-0.67	0.85	-4.79	-4.47	0.32
C _{2v} -C ₈₀ (31922)	0.24	-0.92	1.16	0.24	-0.89	1.13	-5.02	-4.22	0.80
C ₅ -C ₈₂ (39715)	0.19	-0.98	1.17	0.35	-0.96	1.31	-4.98	-4.16	0.82
C _{3v} -C ₈₂ (39717)	0.45	-1.19	1.64	0.54	-1.17	1.71	-5.19	-3.96	1.23
C _{2v} -C ₈₄ (51575)	0.24	-1.06	1.30	-	-	-	-5.01	-4.09	0.92
C ₁ -C ₈₄ (51580)	0.12	-1.14	1.26	-	-	-	-4.89	-3.99	0.91

a) All redox potentials are given in V and orbital energies in eV; computed values in o-dichlorobenzene.

To predict the experimental reduction (or oxidation) potentials of Sc₂O@C_{2n}, their “absolute” reduction (or oxidation) potentials are first computed and then made relative to the normal hydrogen electrode (NHE), which has an estimated absolute reduction potential of +4.28 eV, value determined by Cramer and co-workers.[81] The reduction potential E° of process (1) is related to its free energy change ΔG° by the Nernst equation.



Similarly, the oxidation process is associated to process (2)



The electrochemical measurements (cyclic voltammeteries) are in general performed in a solution of o-dichlorobenzene (o-dcb). Therefore, solvation effects were taken into account by means of the continuum conductor-like screening model (COSMO) using o-dcb as solvent. If solvent effects are not included in the calculations, that is, gas phase calculations, meaningless predictions for reduction (and oxidation) potentials are obtained since the charged species, Sc₂O@C_{2n}⁻ and Sc₂O@C_{2n}⁺ are not well described in absence of their environment (solvent + counterions).

Table 7 collects the first anodic and cathodic potentials referenced versus the ferrocenium/ferrocene (Fc⁺/Fc) potential. It has been observed that the electronic component of the free energy, that is, the reduction and electronic energies are able to describe rather well the redox properties of endohedral fullerenes.[82] This is important because the calculations of the harmonic frequencies are rather expensive. Calculated redox potentials in Table 7 are obtained from the reduction and oxidation energies. As expected from the low LUMOs of fullerene cages the energies associated to the reduction process are computed to be rather exothermic (between -3.4 and -4.0 eV). Consequently, the reduction potentials for endohedral fullerenes appear at not very negative potentials despite the electron transfer from the internal cluster to the carbon cage. HOMO and LUMO are mainly localized on the carbon cage and consequently the computed redox potentials correlates very well with the energy of the HOMO and LUMO computed in o-dcb (see Figure 9). This figure also shows that the deviation of the computed reduction potential with respect to the observed values is very small (< 50 mV). However, for

the first oxidation potential the deviation is larger (> 100 mV), indicating that the HOMOs are systematically computed above the real value, even though the shift is not very important. In endohedral metallofullerenes, cyclic voltammetry is an essential technique in the characterization of the different isomers. In particular, the excellent agreement between experimental and theoretical values allows one to discard many isomers when the X-ray structure is unknown.

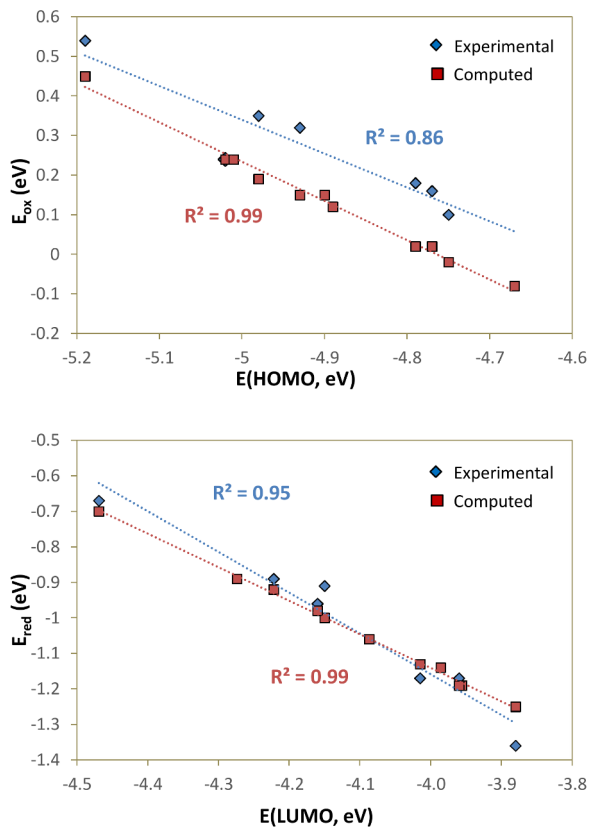


Figure 9. Correlations between first oxidation potentials and HOMO energies (top) and between first reduction potentials and LUMO energies (bottom) for the series of OCFs given in Table 7. Blue diamonds are used for experimental potentials whereas orange squares are for computed potentials.

As shown in Figure 10, the energies of HOMO and LUMO of a given OCF and therefore their redox properties do not correlate with the size of the fullerene. In fact, they are related to the topology of the carbon cage. It was established from the initial studies on the endohedral metallofullerenes that cage $C_{2v}\text{-}C_{82}(39717)$ has an optimal topology to encapsulate clusters or metal ions that involve the transfer of 4 electrons.[83] Thus, $\text{Sc}_2\text{O}@C_{2v}\text{-}C_{82}(39717)$ exhibits an electronic structure with a very deep HOMO and a rather high LUMO, features that are at the origin of the observed electrochemical gap (1.71 eV), which is the largest among the $\text{Sc}_2\text{O}@C_{2n}$ series. In the opposite side, there is $\text{Sc}_2\text{O}@D_{3h}\text{-}C_{78}(24109)$, that is an OCF with a cage that was initially detected hosting Sc_3N . The low energy of the LUMO for this OCF is a result of its electronic structure that is optimal for a 6-electron transfer. Accepting only 4e, $D_{3h}\text{-}C_{78}(24109)$ is in some way an “electron deficient” species being able to be reduced at low potentials. In this line, it is worth mentioning that its second reduction potential (${}^{\text{Red}}E_2$) was found at -0.86 V (vs $\text{Fc}^{0/+}$), only 0.19 V more negative than ${}^{\text{Red}}E_1$, suggesting that it is a system that can easily accept two electrons. Despite the small HOMO-LUMO gap, $\text{Sc}_2\text{O}@D_{3h}\text{-}C_{78}(24109)$ could be isolated and

its structure characterized by X-ray.[22] Among the endohedral fullerenes not yet observed, there is $\text{Sc}_2\text{O}@C_5\text{-}C_{72}$ (10528), which is predicted to have a relative large HOMO-LUMO gap and therefore a presumably important stability. Although this cage has been observed encapsulating the homologous scandium sulfide, it has not been detected as scandium oxide yet. We presume that in the near future $\text{Sc}_2\text{O}@C_5\text{-}C_{72}$ (10528) will likely be isolated and characterized.

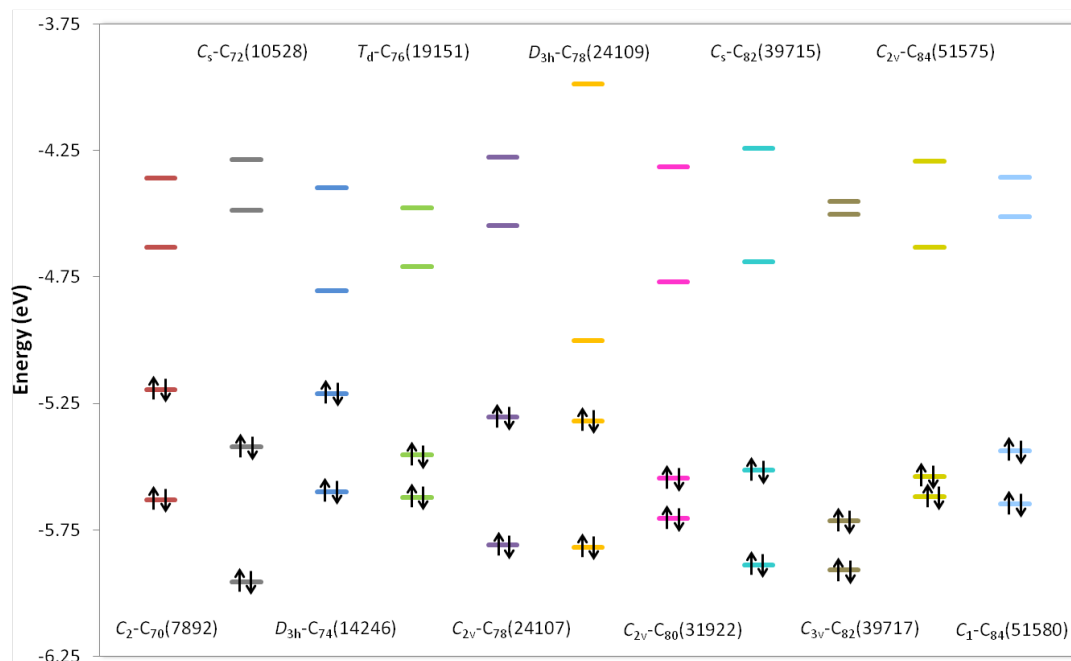


Figure 10. Frontier molecular orbitals for several $\text{Sc}_2\text{O}@C_{2n}$ fullerenes. Energies in eV were computed at gas phase.

5. ^{45}Sc NMR studies of scandium oxide clusterfullerenes

The ^{45}Sc NMR spectra of $\text{Sc}_2\text{O}@C_{2n}$ ($n=35,38,79,40,41$) have been measured at room temperature. As shown in Table 8, up to date, all the reported dimetallic OCFs exhibit a single ^{45}Sc signal, indicating the two Sc ions inside these OCFs either are equivalent or undergo fast rotation inside the cage at the measured temperature. This observation is different from those of the dimetallic carbide CFs, in which $\text{Sc}_2\text{C}_2@C_{2v}\text{-}C_{80}$ (31922) and $\text{Sc}_2\text{C}_2@C_5(39715)\text{-}C_{82}$, present two ^{45}Sc signals with different chemical shifts respectively.[35] [84] This difference suggests that the cluster-cage interactions are similar within the OCF family but they are different from some of the CCFs. On the other hand, the ^{45}Sc chemical shift values obtained for OCFs are widely distributed and there is no evident trend that can be observed from the summary of current data. The ^{45}Sc chemical shift of 32.4 ppm for $\text{Sc}_2\text{O}@C_2\text{-}C_{70}$ (7892) is close to 39.2 ppm for $\text{Sc}_2\text{O}@C_{2v}\text{-}C_{80}$ (31922), even though their cage size are dramatically different. On the contrary, the two isomers of $\text{Sc}_2\text{O}@C_{78}$, $\text{Sc}_2\text{O}@C_{2v}\text{-}C_{78}$ (24107) and $\text{Sc}_2\text{O}@D_{3h}\text{-}C_{78}$ (24109), present significantly different ^{45}Sc chemical shift values of 115 and 90.6 ppm respectively, even though they have same identical cage size and these two cage structures are closely related by a SW transformation.[22] Thus, though no general rule was concluded yet, the summary of the current data clearly shows that the chemical shift of the endohedral Sc atom for dimetallic OCFs is very sensitive to the cage structures.

Due to the different oxide cluster structure, $\text{Sc}_4\text{O}_2@I_h\text{-}C_{80}$ (31924) presents a very different ^{45}Sc NMR spectrum from those of the dimetallic OCFs, in which two peaks at 129/138 and 292/285 ppm were detected respectively. This result agrees well with the fact that the Sc_4O_2 has two

pairs of atoms in Sc^{II} and Sc^{III} valence states. The four different ⁴⁵Sc values also suggest that, though the Sc₄O₂ cluster could rotate freely inside the cage, this cluster is rigid and the four Sc atoms do not arrange within the two faces of the Sc₄ tetrahedron.[49]

Table 8. ⁴⁵Sc NMR chemical shifts in scandium-based oxide endohedral cluster fullerenes (OCFs).

OCF	$\delta(\text{Sc}^{\text{II}})$	$\delta(\text{Sc}^{\text{III}})$	ref
Sc ₂ O@C ₂ -C ₇₀ (7892)		32.4	[45]
Sc ₂ O@T _d -C ₇₆ (19151)		76.9 ^a	[46]
Sc ₂ O@C _{2v} -C ₇₈ (24107)		115.7	[22]
Sc ₂ O@D _{3h} -C ₇₈ (24109)		90.6	[22]
Sc ₂ O@C _{2v} -C ₈₀ (31922)		39.2	[21]
Sc ₂ O@C _{3v} -C ₈₂ (39715)		66.2	[20]
Sc ₄ O ₂ @I _h -C ₈₀ (31924)	292/285	129/138	[49]

6. Conclusions

Despite arc-discharge of graphite is a rather chaotic and violent process, technology has used it for the synthesis of carbon nanofoms such as fullerenes, carbon nanotubes or endo or exo substituted fullerenes during more than 30 years. Burning of graphite rods packed with Sc₂O₃ powders has allowed to synthesize and characterize an important number of scandium oxide fullerenes. In particular, the small Sc₂O cluster has demonstrated to be an excellent template to build around it a carbon cage, especially with a number of carbon atoms between 70 and 82. On the other hand, Sc₄O₃@C₈₀ is the cluster fullerene containing the largest number of internal atoms. Here, the relatively strong bond between trivalent scandium ions and oxide ligands must play an important role in the formation scandium oxide metallofullerenes. Undoubtedly, the relatively large family of endohedral metallofullerenes will significantly increase in the next years and we are persuaded that their synthesis, characterization and functionalization will be useful from a pure scientific perspective, but also for applications in materials and life sciences.

Computational Details

We have computed all the tetraanions of C₇₄ with two or less adjacent pentagon pairs (APP) using density functional theory (DFT) methodology with the ADF 2012 program.[85, 86] The exchange-correlation functional of Becke and Perdew (BP86) and the Slater TZP basis sets were used.[87, 88] Oxidation and reduction potentials were calculated at BP86/TZP level with the inclusion of solvent effects by means of the continuous conductor-like screening model (COSMO).[89, 90] To define the cavity that surrounds the molecules we use the solvent-excluding surface (SES) method and a fine tesserae. The radii of the atoms, which define the dimensions of the cavity surrounding the molecule, were chosen to be 2.00 Å for Sc, 1.52 Å for O and 1.70 Å for C. The dielectric constant was set to 9.8 so as to model o-dichlorobenzene as solvent. The rest of OCFs presented in this review have been already published in previous papers (see references). All of them, but Sc₂O@C₇₀, Sc₂O@C₇₈ and Sc₂O@C₈₄ systems,[22, 45, 91] were computed using the abovementioned methodology. Sc₂O@C₇₀, Sc₂O@C₇₈ and Sc₂O@C₈₄ have been recomputed here at the same theoretical level (BP86/TZP) to be able to compare them with the other systems. Structures and some electronic data for relevant species are available in <http://dx.doi.org/10.19061/iochem-bd-2-17>. For more information about ioChem-

BD see <http://www.iochem-bd.org/>. [92] Molecular dynamics simulations were carried out using Car-Parrinello Molecular Dynamics (CPMD) program. [93] The description of the electronic structure was based on the expansion of the valence electronic wave functions into a plane wave basis set, which was limited by an energy cutoff of 70 Ry. The interaction between the valence electrons and the ionic cores was treated through the pseudopotential (PP) approximation (Martins-Troullier type). [94] The functional by Perdew, Burke and Ernzerhoff (PBE) was selected as density functional. [95, 96] The simulations were carried out using periodic boundary conditions in a cubic cell with a side length of 15 Å, a fictitious electron mass of 800 a.u. and a time step of 0.144 fs. We also used the CaGe code to generate fullerenes. [97]

AUTHOR INFORMATION

Corresponding Authors

*Email: antonio.rodriquezf@urv.cat

*Email: chenning@suda.edu.cn

*Email: josepmaria.poblet@urv.cat

ACKNOWLEDGEMENTS

This work was supported by the Spanish Ministerio de Ciencia e Innovación (Project No. CTQ2014-52774-P) and the Generalitat de Catalunya (2014SGR-199 and XRQTC). J.M.P thanks the ICREA foundation for an ICREA ACADEMIA award. L.A. thanks the Generalitat de Catalunya for a predoctoral fellowship (FI-DGR 2014). N.C thanks for the support by National Science Foundation China (No. 51302178).

REFERENCES

- [1] H.W. Kroto, J.R. Heath, S.C. O'Brien, R.F. Curl, R.E. Smalley, *Nature*, 318 (1985) 162-163.
- [2] W. Kratschmer, L.D. Lamb, K. Fostiropoulos, D.R. Huffman, *Nature*, 347 (1990) 354-358.
- [3] R.B. Ross, C.M. Cardona, D.M. Guldi, S.G. Sankaranarayanan, M.O. Reese, N. Kopidakis, J. Peet, B. Walker, G.C. Bazan, E. Van Keuren, B.C. Holloway, M. Drees, *Nat. Mater.*, 8 (2009) 208-212.
- [4] D.S. Bethune, R.D. Johnson, J.R. Salem, M.S. de Vries, C.S. Yannoni, *Nature*, 366 (1993) 123-128.
- [5] Y. Shao, Z. Xiao, C. Bi, Y. Yuan, J. Huang, *Nat. Commun.*, 5 (2014) 5784.
- [6] P.-W. Liang, C.-C. Chueh, S.T. Williams, A.K.Y. Jen, *Adv. Energy Mater.*, 5 (2015) 1402321.
- [7] Y. Li, Y. Zhao, Q. Chen, Y.M. Yang, Y. Liu, Z. Hong, Z. Liu, Y.T. Hsieh, L. Meng, Y. Yang, *J. Am. Chem. Soc.*, 137 (2015) 15540-15547.
- [8] W. Ke, D. Zhao, C.R. Grice, A.J. Cimaroli, J. Ge, H. Tao, H. Lei, G. Fang, Y. Yan, *J. Mater. Chem. A*, 3 (2015) 17971-17976.
- [9] C.-Y. Chang, W.-K. Huang, Y.-C. Chang, K.-T. Lee, C.-T. Chen, *J. Mater. Chem. A*, 4 (2016) 640-648.
- [10] S.G. Kang, G. Zhou, P. Yang, Y. Liu, B. Sun, T. Huynh, H. Meng, L. Zhao, G. Xing, C. Chen, Y. Zhao, R. Zhou, *Proc. Natl. Acad. Sci. U. S. A.*, 109 (2012) 15431-15436.
- [11] J.F. Zhang, P.P. Fatouros, C.Y. Shu, J. Reid, L.S. Owens, T. Cai, H.W. Gibson, G.L. Long, F.D. Corwin, Z.J. Chen, H.C. Dorn, *Bioconjug. Chem.*, 21 (2010) 610-615.
- [12] H. Yang, M. Yu, H. Jin, Z. Liu, M. Yao, B. Liu, M.M. Olmstead, A.L. Balch, *J. Am. Chem. Soc.*, 134 (2012) 5331-5338.

- [13] H. Yang, H. Jin, X. Wang, Z. Liu, M. Yu, F. Zhao, B.Q. Mercado, M.M. Olmstead, A.L. Balch, J. Am. Chem. Soc., 134 (2012) 14127-14136.
- [14] M. Suzuki, Z. Slanina, N. Mizorogi, X. Lu, S. Nagase, M.M. Olmstead, A.L. Balch, T. Akasaka, J. Am. Chem. Soc., 134 (2012) 18772-18778.
- [15] W. Xu, Y. Hao, F. Uhlík, Z. Shi, Z. Slanina, L. Feng, Nanoscale, 5 (2013) 10409-10413.
- [16] J.P. Martinez, M. Garcia-Borras, S. Osuna, J. Poater, F.M. Bickelhaupt, M. Sola, Chem. Eur. J., 22 (2016) 5953-5962.
- [17] L. Bao, M. Chen, C. Pan, T. Yamaguchi, T. Kato, M.M. Olmstead, A.L. Balch, T. Akasaka, X. Lu, Angew. Chem. Int. Ed. Engl., 55 (2016) 4242-4246.
- [18] Y. Sado, S. Aoyagi, N. Izumi, R. Kitaura, T. Kowalczyk, J. Wang, S. Irle, E. Nishibori, K. Sugimoto, H. Shinohara, Chem. Phys. Lett., 600 (2014) 38-42.
- [19] T. Wei, S. Wang, F. Liu, Y. Tan, X. Zhu, S. Xie, S. Yang, J. Am. Chem. Soc., 137 (2015) 3119-3123.
- [20] Q. Tang, L. Abella, Y. Hao, X. Li, Y. Wan, A. Rodríguez-Forteza, J.M. Poblet, L. Feng, N. Chen, Inorg. Chem., 55 (2016) 1926-1933.
- [21] Q. Tang, L. Abella, Y. Hao, X. Li, Y. Wan, A. Rodríguez-Forteza, J.M. Poblet, L. Feng, N. Chen, Inorg. Chem., 54 (2015) 9845-9852.
- [22] Y. Hao, Q. Tang, X. Li, M. Zhang, Y. Wan, L. Feng, N. Chen, Z. Slanina, L. Adamowicz, F. Uhlík, Inorg. Chem., 55 (2016) 11354-11361.
- [23] Y. Wang, Q. Tang, L. Feng, N. Chen, Inorg. Chem., 56 (2017) 1974-1980.
- [24] C.-H. Chen, L. Abella, M.R. Cerón, M.A. Guerrero-Ayala, A. Rodríguez-Forteza, M.M. Olmstead, X.B. Powers, A.L. Balch, J.M. Poblet, L. Echegoyen, J. Am. Chem. Soc., 138 (2016) 13030-13037.
- [25] A. Krachmalnicoff, R. Bounds, S. Mamone, S. Alom, M. Concistrè, B. Meier, K. Kouřil, M.E. Light, M.R. Johnson, S. Rols, A.J. Horsewill, A. Shugai, U. Nagel, T. Rööm, M. Carravetta, M.H. Levitt, R.J. Whitby, Nat. Chem., 8 (2016) 953-957.
- [26] F.-F. Li, N. Chen, M. Mulet-Gas, V. Triana, J. Murillo, A. Rodríguez-Forteza, J.M. Poblet, L. Echegoyen, Chem. Sci., 4 (2013) 3404.
- [27] T. Wei, S. Wang, X. Lu, Y. Tan, J. Huang, F. Liu, Q. Li, S. Xie, S. Yang, J. Am. Chem. Soc., 138 (2016) 207-214.
- [28] K. Junghans, C. Schlesier, A. Kostanyan, N.A. Samoylova, Q. Deng, M. Rosenkranz, S. Schiemenz, R. Westerstrom, T. Greber, B. Buchner, A.A. Popov, Angew. Chem. Int. Ed. Engl., 54 (2015) 13411-13415.
- [29] Y. Zhang, A.A. Popov, S. Schiemenz, L. Dunsch, Chem. Eur. J., 18 (2012) 9691-9698.
- [30] R. Westerstrom, J. Dreiser, C. Piamonteze, M. Muntwiler, S. Weyeneth, H. Brune, S. Rusponi, F. Nolting, A. Popov, S. Yang, L. Dunsch, T. Greber, J. Am. Chem. Soc., 134 (2012) 9840-9843.
- [31] S. Stevenson, C.B. Rose, J.S. Maslenikova, J.R. Villarreal, M.A. Mackey, B.Q. Mercado, K. Chen, M.M. Olmstead, A.L. Balch, Inorg. Chem., 51 (2012) 13096-13102.
- [32] W. Fu, L. Xu, H. Azurmendi, J. Ge, T. Fuhrer, T. Zuo, J. Reid, C. Shu, K. Harich, H.C. Dorn, J. Am. Chem. Soc., 131 (2009) 11762-11769.
- [33] J.C. Duchamp, A. Demortier, K.R. Fletcher, D. Dorn, E.B. Iezzi, T. Glass, H.C. Dorn, Chem. Phys. Lett., 375 (2003) 655-659.
- [34] Y. Feng, T. Wang, J. Wu, L. Feng, J. Xiang, Y. Ma, Z. Zhang, L. Jiang, C. Shu, C. Wang, Nanoscale, 5 (2013) 6704-6707.
- [35] H. Kurihara, X. Lu, Y. Iiduka, N. Mizorogi, Z. Slanina, T. Tsuchiya, T. Akasaka, S. Nagase, J. Am. Chem. Soc., 133 (2011) 2382-2385.
- [36] H. Kurihara, X. Lu, Y. Iiduka, H. Nikawa, M. Hachiya, N. Mizorogi, Z. Slanina, T. Tsuchiya, S. Nagase, T. Akasaka, Inorg. Chem., 51 (2012) 746-750.
- [37] X. Lu, K. Nakajima, Y. Iiduka, H. Nikawa, T. Tsuchiya, N. Mizorogi, Z. Slanina, S. Nagase, T. Akasaka, Angew. Chem. Int. Ed., 51 (2012) 5889-5892.

- [38] H. Kurihara, X. Lu, Y. Iiduka, N. Mizorogi, Z. Slanina, T. Tsuchiya, S. Nagase, T. Akasaka, *Chem. Commun. (Camb)*, 48 (2012) 1290-1292.
- [39] C.-H. Chen, K.B. Ghiassi, M.R. Cerón, M.A. Guerrero-Ayala, L. Echegoyen, M.M. Olmstead, A.L. Balch, *J. Am. Chem. Soc.*, 137 (2015) 10116-10119.
- [40] M. Krause, F. Ziegls, A.A. Popov, L. Dunsch, *ChemPhysChem*, 8 (2007) 537-540.
- [41] S. Yang, C. Chen, F. Liu, Y. Xie, F. Li, M. Jiao, M. Suzuki, T. Wei, S. Wang, Z. Chen, X. Lu, T. Akasaka, *Sci. Rep.*, 3 (2013) 1487.
- [42] N. Chen, M.N. Chaur, C. Moore, J.R. Pinzon, R. Valencia, A. Rodriguez-Forteza, J.M. Poblet, L. Echegoyen, *Chem. Commun. (Camb)*, 46 (2010) 4818-4820.
- [43] N. Chen, C.M. Beavers, M. Mulet-Gas, A. Rodríguez-Forteza, E.J. Munoz, Y.-Y. Li, M.M. Olmstead, A.L. Balch, J.M. Poblet, L. Echegoyen, *J. Am. Chem. Soc.*, 134 (2012) 7851-7860.
- [44] N. Chen, M. Mulet-Gas, Y.Y. Li, R.E. Stene, C.W. Atherton, A. Rodriguez-Forteza, J.M. Poblet, L. Echegoyen, *Chem. Sci.*, 4 (2013) 180-186.
- [45] M. Zhang, Y. Hao, X. Li, L. Feng, T. Yang, Y. Wan, N. Chen, Z. Slanina, F. Uhlík, H. Cong, *J. Phys. Chem. C*, 118 (2014) 28883-28889.
- [46] T. Yang, Y. Hao, L. Abella, Q. Tang, X. Li, Y. Wan, A. Rodriguez-Forteza, J.M. Poblet, L. Feng, N. Chen, *Chem. Eur. J.*, 21 (2015) 11110-11117.
- [47] S. Stevenson, M.A. Mackey, M.A. Stuart, J.P. Phillips, M.L. Easterling, C.J. Chancellor, M.M. Olmstead, A.L. Balch, *J. Am. Chem. Soc.*, 130 (2008) 11844-11845.
- [48] S. Stevenson, G. Rice, T. Glass, K. Harich, F. Cromer, M.R. Jordan, J. Craft, E. Hadju, R. Bible, M.M. Olmstead, K. Maitra, A.J. Fisher, A.L. Balch, H.C. Dorn, *Nature*, 401 (1999) 55-57.
- [49] A.A. Popov, N. Chen, J.R. Pinzon, S. Stevenson, L.A. Echegoyen, L. Dunsch, *J. Am. Chem. Soc.*, 134 (2012) 19607-19618.
- [50] B.Q. Mercado, N. Chen, A. Rodriguez-Forteza, M.A. Mackey, S. Stevenson, L. Echegoyen, J.M. Poblet, M.M. Olmstead, A.L. Balch, *J. Am. Chem. Soc.*, 133 (2011) 6752-6760.
- [51] L. Abella, Q. Tang, X. Zhang, Y. Wang, N. Chen, J.M. Poblet, A. Rodríguez-Forteza, *J. Phys. Chem. C*, 120 (2016) 26159-26167.
- [52] Q.L. Zhang, S.C. O'Brien, J.R. Heath, Y. Liu, R.F. Curl, H.W. Kroto, R.E. Smalley, *J. Phys. Chem.*, 90 (1986) 525-528.
- [53] R.E. Smalley, *Acc. Chem. Res.*, 25 (1992) 98-105.
- [54] H. Schwarz, *Angew. Chem. Int. Ed. in English*, 32 (1993) 1412-1415.
- [55] Y. Ueno, S. Saito, *Phys. Rev. B*, 77 (2008).
- [56] T. Wakabayashi, Y. Achiba, *Chem. Phys. Lett.*, 190 (1992) 465-468.
- [57] S. Irle, G. Zheng, Z. Wang, K. Morokuma, *J. Phys. Chem. B*, 110 (2006) 14531-14545.
- [58] B. Saha, S. Irle, K. Morokuma, *J. Phys. Chem. C*, 115 (2011) 22707-22716.
- [59] A.S. Fedorov, D.A. Fedorov, A.A. Kuzubov, P.V. Avramov, Y. Nishimura, S. Irle, H.A. Witek, *Phys. Rev. Lett.*, 107 (2011).
- [60] R.F. Curl, M.K. Lee, G.E. Scuseria, *J. Phys. Chem. A*, 112 (2008) 11951-11955.
- [61] J. Zhang, F.L. Bowles, D.W. Bearden, W.K. Ray, T. Fuhrer, Y. Ye, C. Dixon, K. Harich, R.F. Helm, M.M. Olmstead, A.L. Balch, H.C. Dorn, *Nat. Chem.*, 5 (2013) 880-885.
- [62] P.W. Dunk, N.K. Kaiser, C.L. Hendrickson, J.P. Quinn, C.P. Ewels, Y. Nakanishi, Y. Sasaki, H. Shinohara, A.G. Marshall, H.W. Kroto, *Nat. Commun.*, 3 (2012).
- [63] M. Mulet-Gas, L. Abella, P.W. Dunk, A. Rodriguez-Forteza, H.W. Kroto, J.M. Poblet, *Chem. Sci.*, 6 (2015) 675-686.
- [64] P.W. Dunk, N.K. Kaiser, M. Mulet-Gas, A. Rodriguez-Forteza, J.M. Poblet, H. Shinohara, C.L. Hendrickson, A.G. Marshall, H.W. Kroto, *J. Am. Chem. Soc.*, 134 (2012) 9380-9389.
- [65] L.-H. Gan, R. Wu, J.-L. Tian, P.W. Fowler, *Phys. Chem. Chem. Phys.*, 19 (2017) 419-425.
- [66] Y. Zhang, K.B. Ghiassi, Q. Deng, N.A. Samoylova, M.M. Olmstead, A.L. Balch, A.A. Popov, *Angew. Chem. Int. Ed.*, 54 (2015) 495-499.
- [67] B.Q. Mercado, M.A. Stuart, M.A. Mackey, J.E. Pickens, B.S. Confait, S. Stevenson, M.L. Easterling, R. Valencia, A. Rodriguez-Forteza, J.M. Poblet, M.M. Olmstead, A.L. Balch, *J. Am. Chem. Soc.*, 132 (2010) 12098-12105.

- [68] L. Dunsch, S.F. Yang, L. Zhang, A. Svitova, S. Oswald, A.A. Popov, *J. Am. Chem. Soc.*, 132 (2010) 5413-5421.
- [69] Y.-J. Guo, B.-C. Gao, T. Yang, S. Nagase, X. Zhao, *Phys. Chem. Chem. Phys.*, 16 (2014) 15994-16002.
- [70] P. Zhao, T. Yang, Y.-J. Guo, J.-S. Dang, X. Zhao, S. Nagase, *J. Comput. Chem.*, 35 (2014) 1657-1663.
- [71] A. Rodriguez-Forteza, N. Alegret, A.L. Balch, J.M. Poblet, *Nat. Chem.*, 2 (2010) 955-961.
- [72] A. Rodriguez-Forteza, A.L. Balch, J.M. Poblet, *Chem. Soc. Rev.*, 40 (2011) 3551-3563.
- [73] B.Q. Mercado, M.M. Olmstead, C.M. Beavers, M.L. Easterling, S. Stevenson, M.A. Mackey, C.E. Coumbe, J.D. Phillips, J.P. Phillips, J.M. Poblet, A.L. Balch, *Chem. Commun.*, 46 (2010) 279-281.
- [74] T. Wang, J. Wu, Y. Feng, *Dalton Trans.*, 43 (2014) 16270-16274.
- [75] N. Alegret, L. Abella, A. Rodriguez-Forteza, J.M. Poblet, *Theor. Chem. Acc.*, 134 (2015).
- [76] R. Valencia, A. Rodriguez-Forteza, S. Stevenson, A.L. Balch, J.M. Poblet, *Inorg. Chem.*, 48 (2009) 5957-5961.
- [77] A.A. Popov, L. Dunsch, *Chem. Eur. J.*, 15 (2009) 9707-9729.
- [78] A.A. Popov, L. Dunsch, *J. Phys. Chem. Lett.*, 2 (2011) 786-794.
- [79] M.R. Ceron, M. Izquierdo, M. Garcia-Borras, S.S. Lee, S. Stevenson, S. Osuna, L. Echegoyen, *J. Am. Chem. Soc.*, 137 (2015) 11775-11782.
- [80] D.M. Rivera-Nazario, J.R. Pinzón, S. Stevenson, L.A. Echegoyen, *J. Phys. Org. Chem.*, 26 (2013) 194-205.
- [81] A. Lewis, J.A. Bumpus, D.G. Truhlar, C.J. Cramer, *J. Chem. Educ.*, 81 (2004) 596-604.
- [82] R. Valencia, A. Rodriguez-Forteza, A. Clotet, C. de Graaf, M.N. Chaur, L. Echegoyen, J.M. Poblet, *Chem. Eur. J.*, 15 (2009) 10997-11009.
- [83] R. Valencia, A. Rodriguez-Forteza, J.M. Poblet, *J. Phys. Chem. A*, 112 (2008) 4550-4555.
- [84] X. Lu, K. Nakajima, Y. Iiduka, H. Nikawa, N. Mizorogi, Z. Slanina, T. Tsuchiya, S. Nagase, T. Akasaka, *J. Am. Chem. Soc.*, 133 (2011) 19553-19558.
- [85] G. te Velde, F.M. Bickelhaupt, E.J. Baerends, C.F. Guerra, S.J.A. Van Gisbergen, J.G. Snijders, T. Ziegler, *J. Comput. Chem.*, 22 (2001) 931-967.
- [86] E.J.E. Baerends, D. E.; Ros, P., ADF 2012.01, Department of Theoretical Chemistry Vrije Universiteit: Amsterdam, 2012.
- [87] A.D. Becke, *Phys. Rev. A*, 38 (1988) 3098-3100.
- [88] A.D. Becke, *J. Chem. Phys.*, 84 (1986) 4524-4529.
- [89] J. Andzelm, C. Kolmel, A. Klamt, *J. Chem. Phys.*, 103 (1995) 9312-9320.
- [90] A. Klamt, G. Schuurmann, *J. Chem. Soc. Perkin Trans. 2*, (1993) 799-805.
- [91] Y.-J. Guo, X. Zhao, P. Zhao, T. Yang, *J. Phys. Chem. A*, 119 (2015) 10428-10439.
- [92] M. Álvarez-Moreno, C. de Graaf, N. López, F. Maseras, J.M. Poblet, C. Bo, *J. Chem. Inf. Model.*, 55 (2015) 95-103.
- [93] R. Car, M. Parrinello, *Phys. Rev. Lett.*, 55 (1985) 2471-2474.
- [94] N. Troullier, J.L. Martins, *Phys. Rev. B*, 43 (1991) 1993-2006.
- [95] J.P. Perdew, K. Burke, M. Ernzerhof, *Phys. Rev. Lett.*, 77 (1996) 3865-3868.
- [96] J.P. Perdew, K. Burke, M. Ernzerhof, *Phys. Rev. Lett.*, 78 (1997) 1396-1396.
- [97] G. Brinkmann, O. Delgado-Friedrichs, S. Liskin, A. Peeters, N.V. Cleemput, *MATCH Commun. Math. Comput. Chem.*, 63 (2010) 533-552.